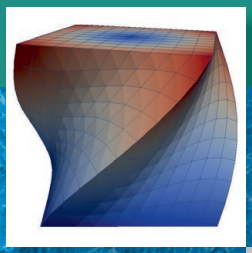

Multiscale modeling and optimization of the mechanics of hierarchical metamaterials

Dennis M. Kochmann, Jonathan B. Hopkins, and Lorenzo Valdevit

We present a survey of modeling techniques used to describe and predict architected cellular metamaterials, and to optimize their topology and geometry toward tailoring their mechanical properties such as stiffness, strength, fracture toughness, and energy absorption. Architectures of interest include truss-, plate-, and shell-based networks with and without periodicity, whose effective mechanical behavior is simulated by tools such as classical finite elements, further scale-bridging techniques such as homogenization and concurrent scale-coupling, and effective continuum descriptions of the underlying discrete networks. In addition to summarizing advances in applying the latter techniques to improve the properties of metamaterials and featuring prominent examples of structure–property relations achieved this way, we also present recently introduced techniques to improve the optimization process toward a full exploitation of the available design space, accounting for both linear and nonlinear material behavior.

Introduction

At the beginnings of metamaterials stood a theoretical prediction[1] regarding negative-refractive-index photonic materials whose experimental realization was to follow only decades later.[2] When it comes to mechanical metamaterials, theoretical-computational predictions also play a significant role in guiding the metamaterial design and optimization process.

Yet, recent accelerated advances in small-scale fabrication[3] have made it challenging for theory and simulations to keep up with the pace of new experimental opportunities. Considerable challenges stem from, among others, (1) the various scales involved[4] (from nanometer-scale features to macroscale samples), (2) the failure of separating material-level from structural-level behavior in small-scale structures,[4–6] (3) the multiphysics nature of the phenomena at play, (4) the tremendous multiscale design space, and (5) the growing importance of imperfections with decreasing length scale.[7] The goal of any modeling approach is the accurate prediction of the effective (meta)materials properties in order to replace expensive trial-and-error experimentation by a simulation-guided exploration and optimization of the design space, as well as to assist in shedding light on the observed physical principles at play. This article focuses on modeling cellular metamaterials (including the broad and popular classes of truss-, plate-, and shell-based architectures), while many of the techniques are widely applicable beyond the scope of this contribution. Further, we treat perfect systems, while imperfections are discussed elsewhere.[7]

Cellular metamaterials are intriguing for a number of reasons. Their low relative density offers lightweight solutions for applications ranging from aerospace and transportation to clothing, medical devices, and personal protection. Large surface-to-volume ratios make them ideal for multiphysics applications such as catalysis, heat exchange, and fluid mixing. Additionally (and essential here), the underlying structural architecture allows simulation approaches pioneered at classical engineering scales without the statistical complications of atomic-scale simulations, which makes for intuitive design guidelines. One may further differentiate between periodic architectures (based on the tessellation of a unit cell, so that modeling techniques may exploit the periodicity and symmetries of the system), aperiodic, random

Dennis M. Kochmann, ETH Zürich, Switzerland; dmk@ethz.ch
Jonathan B. Hopkins, University of California, Los Angeles, USA; hopkins@seas.ucla.edu
Lorenzo Valdevit, University of California, Irvine, USA; valdevit@uci.edu
doi:10.1557/mrs.2019.228

designs[8,9] (whose effective properties are more challenging to extract), as well as quasi-periodic metamaterials (which display periodicity on some scale while featuring randomness on others). Finally, experimental techniques have facilitated multiscale cellular architectures with features spanning from a few nanometers to microns to many centimeters,[4] allowing for design optimization across many levels. This calls for multiscale modeling and optimization strategies that bridge scales, many of which are reviewed in the following.

Effective properties prediction

Analytical approaches

A number of important mechanical properties of architected materials with relatively simple topologies can be treated by analytical approaches. If a periodic truss-based lattice material (e.g., the octet lattice[10]) can be approximated as a network of structural elements (trusses or beams) connected by ideal nodes, then its effective elastic stiffness along different loading directions can be calculated by solving mechanical equilibrium and compatibility equations; similarly, its effective strength can be estimated by relating the macroscale external stress applied to the lattice to the loads carried by each strut, and adopting a yield, fracture, or elastic buckling failure condition at the strut level. This technique has been successfully applied to a number of periodic lattice topologies[10–14] as well as to stochastic foams;[11] in the latter case, analytical solutions provide the scaling of stiffness and strength with relative density, but absolute values require the fitting of nondimensional constants of order one to experiments or numerical simulations.

More recently, analytical techniques have been extended to plate-based closed-cell periodic architected materials to derive necessary conditions that guarantee elastic isotropy.[15] Furthermore, analytical techniques have been used to extract the effective initial fracture toughness of truss-based cellular materials and foams, and to elucidate the dependence of toughness on relative density, fracture strength of individual struts, and unit-cell size. Also in this case, nondimensional constants of order one are fitted to experiments or simulations.[16] More complex material behavior can be described by methods of homogenization to extract the linear, nonlinear, or dynamic metamaterial response from averaging over a representative unit cell—this includes both the determination of effective material behavior[10,17–20] (such as the stress–strain response) as well as multiscale simulations in which the constitutive behavior on the macroscale is computed on the fly by solving a nested lower-scale problem at the unit cell level. The latter approach can also describe localization and size-dependent phenomena,[21] but may require semi-analytical or numerical solution schemes.

Multiple studies using the previously mentioned techniques have unveiled key features of lattice materials:[16] (1) a sufficient coordination number (number of bars meeting at a node) must exist for the lattice to carry loads primarily by tension or compression of its members (stretching-dominated lattice). When this condition is satisfied, the lattice is mechanically efficient, with stiffness and strength scaling linearly with the relative density; a key example is the octet lattice. Conversely, when this condition is not satisfied, the lattice carries load by bending of its members (bending-dominated lattice), and its stiffness and strength scale with higher powers of relative density (2 and 3/2, respectively). (2) Most stochastic foams are bending-dominated, and hence mechanically inefficient compared to stretching-dominated periodic lattices. (3) The fracture toughness of truss-based lattice materials and foams scales with the square root of the unit-cell size and a topology-dependent power of the relative density, ranging between 1/2 and 2 (the scaling power is 1 for the octet lattice).

Analytical predictions for stiffness, strength, and fracture toughness have been verified against experiments and numerical simulations and have proven to be remarkably accurate for lattices with solid cross sections at relatively low relative densities.[10,11,13,14,22–24] As the relative density is increased and the thickness-to-diameter ratio of hollow truss lattices is decreased, the aspect ratio of the members (length-to-diameter ratio) is reduced, ultimately violating the slender-strut assumptions underlying such calculations.[25,26] To address these challenges, numerical techniques are required. The same applies to plate- and shell-based architectures, which, in principle, follow similar scaling laws; yet, their structural response cannot easily be described by analytical approaches, so that numerical techniques have become the primary method of choice.

Numerical approaches

Finite element analysis of the unit-cell response

Numerical techniques such as the finite element (FE) method are popular approaches in situations where the effective properties can be extracted from a periodic unit cell, but are not within analytical reach. The first step in FE analysis is mesh generation. Unit cells of architected materials have been meshed with truss, beam, shell, and solid elements, depending on the topology and geometry of the unit cell and the desired compromise between computational speed and accuracy. Except for trivial topologies, the unit cell is generated by computer-aided design (CAD) and subsequently meshed in an FE package or via a dedicated mesh generator.[13] For situations in which commercial CAD packages are unable to accurately resolve important geometrical features (e.g., the shape of a filleted node in a hollow lattice with stout members), custom-built parametric geometry generators have been developed, which offer the additional benefit of seamless integration with geometry optimizers (albeit at the expense of generality).[25]

Recently, stochastic shell-based architected materials with spinodal topologies were shown to possess excellent mechanical properties while being, in principle, amenable to self-assembly by a variety of processing routes. For such topologies, periodic unit cells were generated by solving the Cahn–Hilliard equation for spinodal phase separation for given average phase volume fractions. Interfaces between the resulting spinodal phases were extracted by level-set

or image-processing techniques. This approach has generated both isotropic[27] and anisotropic[28] topologies, by suitable choice of a potential energy landscape. Spinodal topologies are characterized by a uniform negative Gaussian curvature, which enables a more efficient distribution of local stresses upon external loading than for lattice-based materials (**Figure 1**a).

When long-range effects such as buckling and bifurcation are of no concern, properties of periodic architected materials can be extracted from a single unit cell subject to, for example, periodic boundary conditions. These conditions probe the effective response when all unit cells deform in the same manner, hence approximating the response of a periodic infinite architected material undergoing homogeneous deformation. For example, the stiffness tensor can be extracted via numerical homogenization, a procedure relying on an asymptotic expansion of the governing equations, by computing the linearized incremental stress–strain response.[29,30] Application of this approach to truss lattices has demonstrated how classical beam theory indeed applies only in the limit of slender structures, whereas stubby beams and, in particular, hollow-strut architectures require the described numerical treatment to extract the effective mechanics as a function of topology and relative density.[26,31] Recently, similar techniques have been applied to the stiffness tensor of closed-cell plate-based architected materials, which demonstrated that plate-based materials with cubic symmetry exist that are both elastically isotropic and optimally stiff (i.e., they approach the well-known theoretical Hashin–Shtrikman upper bound[32]).

Numerical homogenization has been applied to other linear functional properties (including thermal and electrical conductivity,[29] thermal expansion,[33] and fluid permeability[34]) and also to nonlinear behavior (e.g., the large-deformation response of auxetic architectures [i.e., architectures with a negative Poisson effect][35]).

Unit-cell strength calculations are more challenging, and their accuracy and reliability depend on the chosen definition of strength (e.g., as the onset of yielding, plastic collapse, fracture, or elastic buckling). Moreover, unit-cell results only apply here if the periodicity assumption is adequate (i.e., if localized, aperiodic behavior can be excluded). The onset of yielding is estimated by applying a macroscopic strain to the unit cell along the desired loading direction and extracting the macroscopic stress at which the maximum local stress within the unit cell exceeds the yield strength of the base material (modeled as linear elastic).[25] The onset of elastic buckling is generally obtained by a Bloch-type eigenvalue analysis of a single cell,[25,36] with the constituent material again modeled as linear elastic.

When significant geometric nonlinearities are expected, bifurcation can be triggered by precomputing the effective elastic buckling strength and the associated lowest buckling modes (e.g., from preloading the unit cell up to buckling, followed by an eigenvalue analysis). Once extracted, a linear combination of the first modes can be used to introduce a small geometric imperfection, so that a subsequent simulation of the unit cell until collapse via a nonlinear quasistatic or Riks analysis provides a measure of the elastic/plastic buckling strength of the architected material.[37] Post-buckling simulations are generally able to capture the entire stress–strain response of the material quite reliably, even for complex topologies (Figure 1b). Eigenvalue extractions on unit cells will only capture buckling modes with wavelengths smaller than the unit-cell size. While often these modes dominate the strength, this is not universally true, and larger numbers of unit cells may be required for accurate extraction of the effective buckling strength.[38,39] An alternative technique for elastic buckling strength calculations is based on the Bloch–Floquet theory, which searches for unstable modes of, in principle, arbitrary wavelength.[40–42] This powerful technique allows for an accurate estimation of the lowest buckling modes (and associated strength) for wavelengths longer than the unit-cell size.

The same Bloch wave ansatz is also widely used to predict the response of architected materials to mechanical and acoustic waves,[43–45] enabling the modeling and design of metamaterials with tailored bandgaps for controlled wave attenuation, wave guiding and redirection, or signal processing. Applicable to, in principle, any periodic architecture, the entire space of wave vectors is sampled to extract the wave dispersion relations of the metamaterial, uniquely linking excitation frequencies to wavelengths and directions, and revealing frequencies that do not propagate waves in specific directions (partial bandgaps) or in all

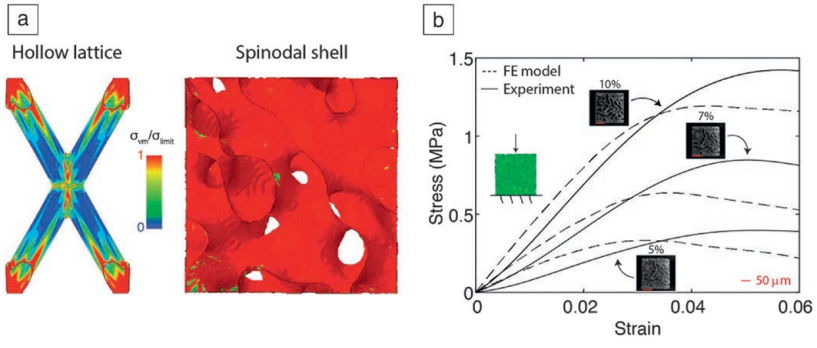

Figure 1. The mechanical performance of spinodal shell-based architected materials. (a) Comparison of the distribution of the local von Mises stress (σ_{VM}) normalized by the limit stress for the materials (σ_{limit}), in a hollow microlattice unit cell and a spinodal shell topology of the same relative density, both loaded under the same macroscopic uniaxial compressive strain. Notice that the uniform negative Gaussian curvature of the spinodal shell results in a more uniform stress distribution and superior mechanical efficiency. (b) Comparison of elastoplastic stress–strain response obtained by uniaxial compression experiments and finite element (FE) modeling. The samples of spinodal shell architectures at three relative densities, displayed in the insets, are produced by two-photon polymerization direct laser writing at the microscale in an acrylate resin and tested with an Alemnis nanoindenter inside a scanning electron microscope.[27]

directions (full bandgaps). Further computing the group velocity from the dispersion surfaces reveals the directions of energy flow in the medium,[46] thus effectively predicting the directions in which vibrational energy will flow—making the approach enabling tailored wave guiding (or wave beaming).

Over the last decade, instabilities have been exploited to create beneficial effective properties.[47] For example, elastic snap-through (i.e., the sudden change of configuration of structural elements as a result of an elastic instability) within carefully designed unit cells upon macroscopic loading has been used as a mechanism to dissipate kinetic energy via the damping of high-frequency vibrations of unit-cell features based on the constituent material's intrinsic damping. When appropriately designed, this mechanism enormously amplifies the intrinsic damping of the base material and can be used to generate single- or multi-stable periodic architected materials with nearly linear elastic constituents, which exhibit exceptional combinations of strength, stiffness and energy dissipation, energy trapping or force isolation.[48–57] **Figure 2** provides an example of this mechanism. Figure 2a shows a laser-cut two-dimensional (2D) periodic architected material, where each unit cell contains rigid elements connected by thin flexible hinges. The analytical prediction of the mechanical response of a single hinge under compression is shown in Figure 2b, which shows the snap-through behavior. The behavior of the architected material consisting of multiple cells is analytically predicted in Figure 2c, as a function of the number of cells. Finally, the experimental response of a sample with seven unit cells is compared to the analytical prediction in Figure 2d. The ability to predict the stress–strain curve of the unit cell during the snap-through (and hence through a regime of negative stiffness) is essential for modeling and designing such architected materials and can be obtained by post-buckling FE analysis at the unit-cell level or by beam theory (Figure 2b–d).[52,53,56]

FE analysis of multicell architected materials

The limits of unit-cell analysis become evident in fracture toughness calculations; the localized presence of a discrete crack in the material violates the assumption of a separation of scales (and hence of the assumed periodic deformation). For the definition of fracture toughness to hold, the sample must be much larger than the crack, which in turn, needs to be much larger than the unit-cell size, making fracture toughness computations for lattices remarkably expensive.

Two key approaches have been successfully used: (1) For 2D brittle lattice materials, a relatively small number of unit cells around the crack tip is meshed with beam elements. The sample is subjected to displacement boundary conditions consistent with the *K*-field solution for a continuum material with the same effective elastic properties as the lattice material, and the largest stress in a strut in the lattice is extracted. The fracture toughness is calculated as the ratio of the constituent material's tensile strength to the largest stress in the lattice, multiplied by the applied value of the stress intensity factor.[16,58–60] (2) A single edge notch bend (SENB) specimen with dimensions consistent with ASTM standards is meshed with a lattice material, generally using beam elements. The sample is loaded in three-point bending, and the load-crack extension curve is extracted. Standard formulas are employed to compute the initial fracture toughness and the resistance (R) curve of the lattice material. This approach has been used for 2D and three-dimensional (3D) lattices, including the octet lattice.[24] Both techniques have been used to validate analytical estimates and calculate the

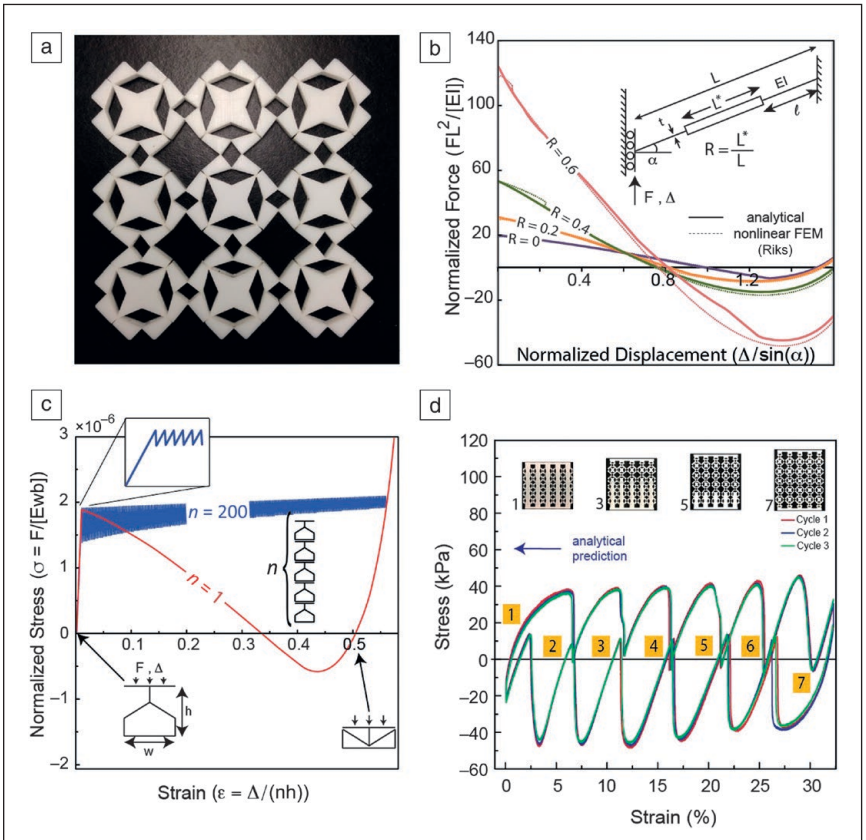

Figure 2. Multistable architected material exploiting negative-stiffness elements. (a) Implementation of the topology. (b) Calculated load-displacement response of a single hinge under displacement control as a function of the geometric parameters of the hinge, showing the region of negative stiffness. The directions of load, F, and displacement, Δ, and the boundary conditions are shown in the inset. Notice that analytical and numerical models agree nearly perfectly. (c) Calculated stress–strain response of the material shown in (a), for a single unit cell and for 200 unit cells in series (approaching the continuum response). Loading direction and geometrical parameters are defined in the inset. (d) Experimental stress–strain response of the material shown in (a), with seven unit cells in series. Notice the significant amount of energy dissipation and hysteresis enabled by negative-stiffness mechanisms.[56] Note: EI, flexural stiffness of the hinge; E, elastic modulus; w, width; b, out-of-plane thickness.

values of topology-specific nondimensional constants that are included in, but not defined by, the analytical models.

Multiscale techniques

Where the effective behavior cannot be extracted from a unit cell, multiscale techniques become the method of choice, which aim toward the accuracy of unit-cell resolution while providing the efficiency of macroscale calculations. One such approach is the quasicontinuum (QC) method, originally introduced for coarse-graining atomistic lattice calculations[61] and later extended to truss lattices.[62–65] Truss-based QC models the full discrete lattice, but introduces kinematic constraints in regions requiring lower resolution (thus retaining the accuracy of individual structural members where needed, while coarsening the description away from those regions into an efficient continuum manner—with both regions being adaptively updated as needed). A prime application is the aforementioned fracture toughness predictions of truss lattices, for which discrete truss-level resolution is required near the crack tip, while large samples are required to apply loading conditions remotely. Here, full resolution is retained at the crack tip (and evolved adaptively based on regions of highest stresses), while an efficient coarsened description is used in the far field, thus enabling simulations of several orders-of-magnitude larger samples than achievable by discrete structural FE calculations. **Figure 3**c–e shows illustrative examples[65] of coarse-grained fracture specimens using the truss QC method with and without adaptive mesh refinement to produce full resolution in regions of interest.

An alternative is to compute the effective local material behavior from a unit cell on the fly and to feed such information into a macroscale FE simulation.[38,66] Owing to the computational expenses of such homogenization-based approaches (incurred by the nested large- and small-scale simulations), their use has been restricted to relatively simple geometries and problems (see Figure 3a–b for an example of a 3D truss replaced by an efficient FE model).

Emergence of size effects

Recent progress in advanced manufacturing has enabled fabrication of architected materials with unit cells at the micron scale and sub-cell geometric features (e.g., truss diameters) at the nanoscale.[67] When made out of metallic and ceramic materials at this scale, interesting metamaterial size effects may emerge. For example, polycrystalline metals with nanoscale grain size can be readily processed, resulting in increased yield strength (Hall–Petch Law) relative to the bulk.[68–70] Similarly, virtually flaw-free ceramic materials approaching the theoretical strength can be produced at those small scales.[4,71–74] Architecting cellular metamaterials with such exceptionally strong nanoscale constituents allows designers to capitalize on these size effects at a large scale (the scale of the architected material). Moreover, interesting new effects may emerge from architectures in which the feature sizes (e.g., strut diameter or length in trusses) are on the same order as the material features (e.g., grain size).

Our ability to predict the processing-specific microstructural evolution of the constituent material and model these size effects has remained highly limited. Likewise, predicting the effective response when material-level and structural-level phenomena cannot be treated separately anymore is a key open challenge: FE analysis (popular for structure-level simulations) does not capture the small-scale material response and microstructure, while atomistic techniques (capable of accurately describing material microstructure and nanoscale mechanisms) cannot be applied to micron-sized unit cells due to computational costs. The integration of modeling techniques that enable the co-design of material and architecture, by combining tools of Integrated Computational Materials Engineering (ICME) with continuum-level modeling and topology optimization, remains a promising, but widely untapped opportunity.

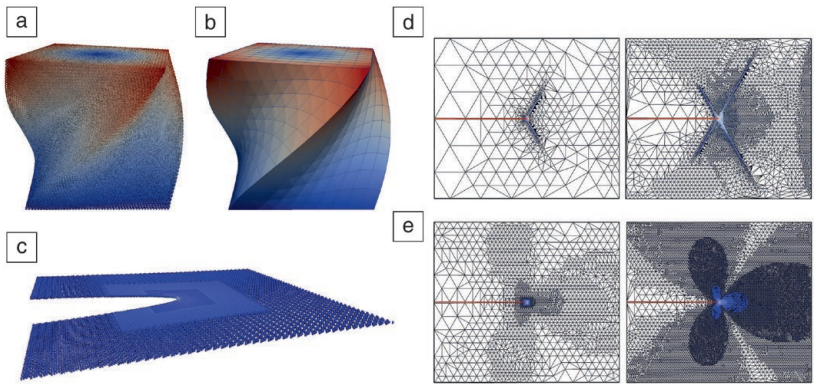

Figure 3. Examples of multiscale modeling approaches for truss metamaterials. Replacing a discrete truss network (a) by a continuum modeled efficiently by finite elements[21] (b) considerably reduces computational costs. The quasicontinuum (QC) method[65] (c) retains full discrete resolution near a crack tip while coarsening away from the notch; mesh adaptivity within the QC method refines locally where stress concentrations are expected in 2D truss lattices made of kagome (d) and triangular (e) unit cells (two sets of graphics visualize the progression of refinement under static loading).

Effective property optimization

Searching the design space of metamaterials to identify optimal concepts that achieve desired effective properties is difficult, given the staggering complexity of microarchitectures and the infinite design space (including the truss-, plate-, and cell-based cellular networks previously discussed). Most computational attempts to systematically design and optimize metamaterials utilize variations of topology or shape optimization,[34,75,76] a detailed review of which is presented in Reference 7. Such approaches typically begin with a random mixture of materials or interconnected beams that are

iteratively removed or altered using genetic algorithms until a metamaterial architecture is identified that more closely achieves the desired properties. Although such approaches often generate impressive nonintuitive designs, they are also computationally expensive and tend to converge to local minima within the design space. Thus, designers have little confidence that a global minimum (i.e., a truly optimal design) has been identified.

Recently, a fundamentally different approach[77] was unveiled to more efficiently search the design space of metamaterials and to increase the chance that a global optimizer is identified. This approach decouples topology synthesis from geometry optimization. Topology synthesis is the process of determining the optimal number, kind, location, and orientation of elements (e.g., beams, notches, or hinges) that constitute the metamaterial's topology. Geometry optimization is the process of determining the optimal geometric parameters (e.g., the optimal lengths, widths, and thicknesses of the constituent beams) that those elements should possess to achieve the desired properties.

To independently perform topology synthesis, the new approach utilizes the mathematics underlying the freedom and constraint topologies (FACT) methodology.[78–80] Using this approach, the topologies of 3D periodic or aperiodic metamaterials can be synthesized with six orders-of-magnitude higher computational efficiency[77] than standard topology optimization approaches. The FACT methodology utilizes a library of geometric spaces that represent every linear combination of independent twist and wrench vectors[81] and embody the complete design space of metamaterial topologies. One set of spaces is called freedom spaces and represents the metamaterial's desired degrees of freedom (DOF). Another set of complementary spaces is called constraint spaces and represents the regions where constraint elements (e.g., beams, notches, and hinges) should be placed within the topology to achieve the desired DOF of their corresponding freedom spaces. Principles have been determined for most efficiently searching the FACT-library's spaces for considering the topology configurations (i.e., parallel,[79,80,82] serial,[83,84] hybrid,[85] and interconnected hybrid[86] configurations) that are likely to yield an optimal topology, which is most promising for achieving the desired properties once its geometry has been optimized. This mathematical framework reduces the amount of information needed to synthesize the topology of metamaterials and affords the approach its synthesis speed.

Once synthesized, the geometric parameters of the elements that constitute the metamaterial's topology are optimized (i.e., geometry optimization is performed independently). To this end, the boundary-learning optimization tool (BLOT)[87] is used, which efficiently leverages machine learning to train a neural network[88] using FE data collected via an automated parameter sweep of the FACT-synthesized topology. Once trained, the neural network model is used within specialized multiobjective optimizers[87] that rapidly identify the boundary of achievable properties. The approach is iterated by adding more FE data, collected along the previously identified boundary, to the neural-network training algorithm until the true boundary, including convex and concave portions, is identified within a specified error percentage.

As an example, we consider a metamaterial that should be stiff in all directions except along two orthogonal compliant directions (e.g., the two translational DOF shown as black arrows in **Figure 4**a)[77] and about an orthogonal compliant rotational axis (e.g., the red rotational DOF line shown with a circular arrow about its axis in Figure 4a). If these three DOF are modeled as twist vectors and are linearly combined, they

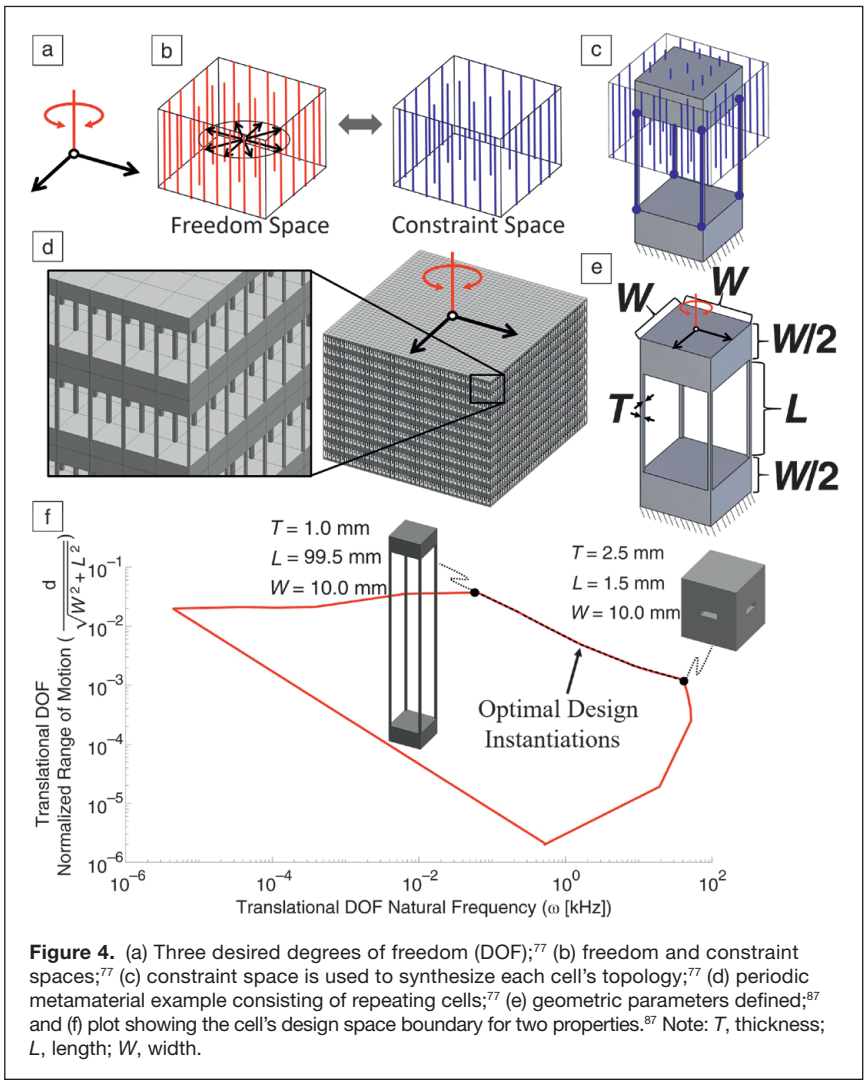

Figure 4. (a) Three desired degrees of freedom (DOF);[77] (b) freedom and constraint spaces;[77] (c) constraint space is used to synthesize each cell's topology;[77] (d) periodic metamaterial example consisting of repeating cells;[77] (e) geometric parameters defined;[87] and (f) plot showing the cell's design space boundary for two properties.[87] Note: *T*, thickness; *L*, length; *W*, width.

generate a freedom space from the complete FACT library of spaces that consists of all translations (shown as the black disk of arrows in Figure 4b) that are perpendicular to the desired rotational axis and all rotational axes that are parallel to that axis (shown as the box of red rotation lines in the same figure). This freedom space uniquely links to the complementary constraint space, also shown in Figure 4b as a box of blue constraint lines parallel to the rotation lines in the freedom space. Each of these constraint lines represents the axis of a potential wire constraint element that would permit the motions within the complementary freedom space. Instructions are embedded in each constraint space within the FACT library to guide the selection of the optimal number and kind of elements from within its geometry. A cell with four parallel wire flexures was synthesized from the constraint space of our example, as shown in Figure 4c. By repeating this cell within a periodic lattice (Figure 4d), the topology of a metamaterial is synthesized that achieves the three desired compliant DOFs shown in Figure 4a.

After the topology is synthesized using the spaces of the FACT library, its geometry can be optimized using the BLOT for any combination of desired properties (e.g., range of translational deformation and natural frequency associated with that DOF). Once the topology's three independent geometric parameters are defined (Figure 4e), the smallest achievable feature sizes for each of these three parameters, as well as the largest geometrically compatible values for the same parameters, must be provided. Examples include the properties of the constituent material as well as the tolerances of the available fabrication process to identify the smallest resolution increment by which each geometric parameter can be changed to sweep between these smallest and largest values. Using this information, the BLOT plots the boundary (Figure 4f) that circumscribes the combination of desired capabilities (e.g., the ranges of motion, d, per system characteristic length, $\sqrt{L^2 + w^2}$, and the natural frequencies, ω, that can be achieved along the direction of the translational DOF by the topology's geometric instantiations for the given range of parameters. Two extreme designs are shown as black dots that lie on either end of the optimal portion of the red boundary plotted in Figure 4f. Note that this approach can optimize for linear and nonlinear properties for any periodic or aperiodic metamaterial topology desired.

Conclusions

The modeling and optimization of metamaterial architectures for tailored mechanical and multifunctional performance can rely on various analytical and computational methods that extract the effective material response from, for instance, unit-cell FE calculations and homogenization approaches, or which involve multiple to many unit cells such as in QC and related multiscale techniques. At smaller scales, discrete and, in particular, atomistic methods gain importance (but require considerable computational resources). Despite many existing approaches, a long list of open challenges remain. These include (1) models for the complex nonlinear, inelastic, and rich nonlinear dynamic response of metamaterials; (2) models for the nano- and microscales where material and structural feature sizes are of the same order and neither classical micromechanical and atomistic techniques nor structural engineering tools are applicable; and (3) sophisticated multiscale techniques that bridge length and time scales. Further challenges arise from the lack of periodicity (such as in self-assembled architectures), where averaging techniques require large representative unit cells and statistical methods gain importance.

When it comes to optimization, techniques are required for more rapidly and intelligently searching the extreme design space, especially for multiphysics properties. Special challenges arise from aperiodic designs, for which the storage and manipulation of billions of nonrepeating constituent elements must be efficiently managed. Finally, accounting for fabrication-based tolerances and imperfections[7] (and assessing the quality of what was actually fabricated) is essential and often neglected when predicting the effective metamaterial performance.

Acknowledgments

D.M.K. acknowledges the support from the Office of Naval Research under Award No. N00014–16–1-2431. J.H.'s work was supported in part by the Air Force Office of Scientific Research under Award No. FA9550–18–1-0459; Program Officer B. Lee is gratefully acknowledged. L.V. acknowledges partial support from the Office of Naval Research under Award No. N00014–11–1-0884 (Program Officer D. Shifler), and the NASA Early Stage Innovation Program under Award No. 80NSSC18K0259.

References

1. V.G. Veselago, *Sov. Phys. Usp.* **10**, 509 (1968).
2. R.A. Shelby, D.R. Smith, S. Shultz, *Science* **292**, 77 (2001).
3. I. Gibson, D.W. Rosen, B. Stucker, *Additive Manufacturing Technologies* (Springer, New York, 2014).
4. L. Meza, A.J. Zelhofer, N. Clarke, A.J. Mateos, D.M. Kochmann, J.R. Greer, *Proc. Natl. Acad. Sci. U.S.A.* **112**, 11502 (2015).
5. X. Li, H. Gao, *Nat. Mater.* **15**, 373 (2016).
6. J.R. Greer, J.T.M. De Hosson, *Prog. Mater. Sci.* **56**, 654 (2011).
7. D. Pasini, J. Guest, *MRS Bull.* **44** (10), 766 (2019).
8. L.J. Gibson, M.F. Ashby, *Cellular Solids: Structure and Properties* (Cambridge University Press, 1999).
9. C. Coulais, E. Teomy, K. de Reus, Y. Shokef, M. van Hecke, *Nature* **535**, 529 (2016).
10. V.S. Deshpande, N.A. Fleck, M.F. Ashby, *J. Mech. Phys. Solids* **49**, 1747 (2001).
11. L. Gibson, M. Ashby, *Cellular Solids: Structure and Properties* (Pergamon Press, Oxford, UK, 1988).
12. N. Wicks, J.W. Hutchinson, *Int. J. Solids Struct.* **38**, 5165 (2001).
13. F.W. Zok, S.A. Waltner, Z. Wei, H.J. Rathbun, R.M. McMeeking, A.G. Evans, *Int J. Solids Struct.* **41**, 6249 (2004).
14. F.W. Zok, H.J. Rathbun, Z. Wei, A.G. Evans, *Int. J. Solids Struct.* **40**, 5707 (2003).
15. T. Tancogne-Dejean, M. Diamantopoulou, M.B. Gorji, C. Bonatti, D. Mohr, *Adv. Mater.* **30**, 1803334 (2018).
16. N.A. Fleck, V.S. Deshpande, M.F. Ashby, *Proc. R. Soc. Lond. A* **466**, 2495 (2011).
17. N. Triantafyllidis, S. Bardenhagen, *J. Elast.* **33**, 259 (1993).
18. Y. Wang, A. Cuitiño, *J. Mech. Phys. Solids* **48**, 961 (2000).
19. J.Y. Chen, Y. Huang, M. Ortiz, *J. Mech. Phys. Solids* **46**, 789 (1998).

20. R.S. Kumar, D.L. McDowell, *Int. J. Solids Struct.* **41**, 7399 (2004).
21. R. Glaesener, C. Lestringant, B. Telgen, D.M. Kochmann, *Int. J. Solids Struct.* **171**, 117 (2019).
22. L. Valdevit, Z. Wei, C. Mercer, F. Zok, A. Evans, *Int. J. Solids Struct.* **43**, 4888 (2006).
23. F.W. Zok, H. Rathbun, M. He, E. Ferri, C. Mercer, R.M. McMeeking, A.G. Evans, *Philos. Mag.* **85**, 3207 (2005).
24. M.R. O'Masta, L. Dong, L. St.-Pierre, H.N.G. Wadley, V.S. Deshpande, *J. Mech. Phys. Solids* **98**, 271 (2016).
25. L. Valdevit, S.W. Godfrey, T.A. Schaedler, A.J. Jacobsen, W.B. Carter, *J. Mater. Res.* **28**, 2461 (2013).
26. L.R. Meza, G. Phlipot, C.M. Portela, A. Maggi, L.C. Montemayor, A. Comella, D.M. Kochmann, J.R. Greer, *Acta Mater.* **140**, 424 (2017).
27. M.-T. Hsieh, B. Endo, Y. Zhang, J. Bauer, L. Valdevit, *J. Mech. Phys. Solids* **125**, 401 (2019).
28. A. Vidyasagar, S. Krödel, D.M. Kochmann, *Proc. R. Soc. Lond. A* **47**, 20180535 (2018).
29. E. Andreassen, C.S. Andreasen, *Comput. Mater. Sci.* **83**, 488 (2014).
30. S. Torquato, *Random Heterogeneous Materials* (Springer, New York, 2002).
31. C.M. Portela, J.R. Greer, D.M. Kochmann. *Extreme Mech. Lett.* **22**, 138 (2018).
32. J.B. Berger, H.N.G. Wadley, R.M. McMeeking, *Nature* **543**, 533 (2017).
33. O. Sigmund, S. Torquato, *J. Mech. Phys. Solids* **45**, 1037 (1997).
34. J.K. Guest, J.H. Prévost, *Int. J. Solids Struct.* **43**, 7028 (2006).
35. D.M. Kochmann, G.N. Venturini, *Smart Mater. Struct.* **22**, 084004 (2013).
36. S. Shan, S.H. Kang, P. Wang, C. Qu, S. Shian, E.R. Chen, K. Bertoldi, *Adv. Funct. Mater.* **24**, 4935 (2014).
37. L. Valdevit, J.W. Hutchinson, A.G. Evans, *Int. J. Solids Struct.* **41**, 5105 (2004).
38. A. Vigliotti, D. Pasini, *Mech. Mater.* **46**, 57 (2012).
39. A. Vigliotti, D. Pasini, *Comput. Methods Appl. Mech. Eng.* **229**, 27 (2012).
40. G. Geymonat, S. Müller, N. Triantafyllidis, *Arch. Ration. Mech. Anal.* **122**, 231 (1993).
41. K. Bertoldi, M.C. Boyce, *Phys. Rev. B* **78**, 184107 (2008).
42. R.G. Hutchinson, N.A. Fleck, *J. Mech. Phys. Solids* **54**, 756 (2006).
43. M.I. Hussein, M.J. Leamy, M. Ruzzene, *Appl. Mech. Rev.* **66**, 040802 (2014).
44. A. Asadpoure, M. Tootkaboni, L. Valdevit, *Comput. Methods Appl. Mech. Eng.* **325**, 314 (2017).
45. L. Salari-Sharif, B. Haghpanah, A. Guell Izard, M. Tootkaboni, L. Valdevit, *Phys. Rev. Appl.* **11**, 024062 (2019).
46. A. Zelhofer, D.M. Kochmann, *Int. J. Solids Struct.* **115–116**, 248 (2017).
47. D.M. Kochmann, K. Bertoldi, *Appl. Mech. Rev.* **69**, 050801 (2017).
48. L. Kashdan, C.C. Seepersad, M. Haberman, P.S. Wilson, *Rapid Prototyp. J.* **18**, 194 (2012).
49. H. Kalathur, R.S. Lakes, *Smart Mater. Struct.* **22**, 084013 (2013).
50. L. Dong, R.S. Lakes, *Int. J. Solids Struct.* **50**, 2416 (2013).
51. D.M. Kochmann. *Mech. Res. Commun.* **58**, 36 (2014).
52. S. Shan, S.H. Kang, J.R. Raney, P. Wang, L. Fang, F. Candido, J.A. Lewis, K. Bertoldi, *Adv. Mater.* **27**, 4296 (2015).
53. K. Bertoldi, V. Vitelli, J. Christensen, M. van Hecke, *Nat. Rev. Mater.* **2**, 17066 (2017).
54. R.L. Harne, K.-W. Wang, *Harnessing Bistable Structural Dynamics: For Vibration Control, Energy Harvesting and Sensing* (Wiley, Chichester, West Sussex, UK, 2017).
55. B. Haghpanah, A. Shirazi, L. Salari-Sharif, A.G. Izard, L. Valdevit, *Extreme Mech. Lett.* **17**, 56 (2017).
56. B. Haghpanah, L. Salari-Sharif, P. Pourrajab, J. Hopkins, L. Valdevit, *Adv. Mater.* **28**, 7915 (2016).
57. A.G. Izard, R.F. Alfonso, G. McKnight, L. Valdevit, *Mater. Des.* **135**, 37 (2017).
58. I. Quintana-Alonso, N.A. Fleck, in *Major Accomplishments in Composite Materials and Sandwich Structures*, I.M. Daniel, E.E. Gdoutos, Y.D.S. Rajapakse, Eds. (Springer, Dordrecht, The Netherlands, 2010), pp. 799–816.
59. H.C. Tankasala, V.S. Deshpande, N.A. Fleck, *J. Appl. Mech.* **82**, 091004 (2015).
60. N.A. Fleck, X. Qiu, *J. Mech. Phys. Solids* **55**, 562 (2007).
61. E.B. Tadmor, M. Ortiz, R. Phillips, *Philos. Mag. A* **73**, 1529 (1996).
62. L.A.A. Beex, R.H.J. Peerlings, M.G.D. Geers, *Int. J. Numer. Methods Eng.* **87**, 701 (2011).
63. L.A.A. Beex, R.H.J. Peerlings, M.G.D. Geers, *J. Mech. Phys. Solids* **64**, 154 (2014).
64. L.A.A. Beex, R.H.J. Peerlings, M.G.D. Geers, *Comput. Methods Appl. Mech. Eng.* **269**, 108 (2014).
65. G.P. Phlipot, D.M. Kochmann, *J. Mech. Phys. Solids* **124**, 758 (2019).
66. A. Vigliotti, V. Deshpande, D. Pasini, *J. Mech. Phys. Solids* **64**, 44 (2014).
67. J. Bauer, L.R. Meza, T.A. Schaedler, R. Schwaiger, X. Zheng, L. Valdevit, *Adv. Mater.* **29**, 1701850 (2017).
68. A. Torrents, T.A. Schaedler, A.J. Jacobsen, W.B. Carter, L. Valdevit, *Acta Mater.* **60**, 3511 (2012).
69. T.A. Schaedler, A.J. Jacobsen, A. Torrents, A.E. Sorensen, J. Lian, J.R. Greer, L. Valdevit, W.B. Carter, *Science* **334**, 962 (2011).
70. A. Vyatskikh, S. Delalande, A. Kudo, X. Zhang, C.M. Portela, J.R. Greer, *Nat. Commun.* **9**, 593 (2018).
71. X. Zhang, A. Vyatskikh, H. Gao, J.R. Greer, X. Li, *Proc. Natl. Acad. Sci. U.S.A.* **116**, 6665 (2019).
72. X. Zhang, L. Zhong, A. Mateos, A. Kudo, A. Vyatskikh, H. Gao, J.R. Greer, X. Li, *Nat. Nanotechnol.* **14**, 762 (2019).
73. L.R. Meza, S. Das, J.R. Greer, *Science* **345**, 1322 (2014).
74. J. Bauer, A. Schroer, R. Schwaiger, I. Tesari, C. Lange, L. Valdevit, O. Kraft, *Extreme Mech. Lett.* **3**, 105 (2015).
75. M. Zhu, Y. Yang, J.K. Guest, M.D. Shields, *Struct. Saf.* **67**, 116 (2017).
76. O. Sigmund, *Mech. Struct. Mach.* **25**, 493 (1997).
77. L.A. Shaw, F. Sun, C.M. Portela, R.I. Barranco, J.R. Greer, J.B. Hopkins, *Nat. Commun.* **10**, 291 (2019).
78. J.B. Hopkins, "Chapter 6: Synthesis Through Freedom and Constraint Topologies," in *Handbook of Compliant Mechanisms*, L.L. Howell, S.P. Magleby, B.M. Olsen, Eds. (Wiley, Oxford, UK, 2013), pp. 79–92.
79. J.B. Hopkins, M.L. Culpepper, *Precis. Eng.* **34**, 259 (2010).
80. J.B. Hopkins, M.L. Culpepper, *Precis. Eng.* **34**, 271 (2010).
81. R.S. Ball, *A Treatise on the Theory of Screws* (Cambridge University Press, Cambridge, UK, 1900).
82. J.B. Hopkins, J.J. Vericella, C.D. Harvey, *Precis. Eng.* **38**, 525 (2014).
83. J.B. Hopkins, M.L. Culpepper, *Precis. Eng.* **35**, 638 (2011).
84. J.B. Hopkins, *J. Mech. Robot.* **7**, 031011 (2015).
85. J.B. Hopkins, *Mech. Sci.* **4**, 319 (2013).
86. F. Sun, J.B. Hopkins, *J. Mech. Robot.* **9**, 031018 (2017).
87. A. Hatamizadeh, Y. Song, J.B. Hopkins, *Math. Probl. Eng.* **2018**, 1058732 (2018).
88. Y. LeCun, Y. Bengio, G. Hinton, *Nature* **521**, 436 (2015). □

Dennis M. Kochmann is professor of mechanics and materials at ETH Zürich, Switzerland, director of the Mechanics and Materials Laboratory and head of the Institute of Mechanical Systems. He received his MS degree from the University of Wisconsin–Madison, and his diploma and doctoral degree from Ruhr-University Bochum, Germany. He completed postdoctoral research at the University of Wisconsin–Madison, and was subsequently a professor of aerospace at the California Institute of Technology. He was a Fulbright and Feodor Lynen Fellow. His awards include the Richard von Mises Prize, the International Congress of Theoretical and Applied Mechanics Bureau Prize in Solid Mechanics, The American Society of Mechanical Engineer's T.J.R. Hughes Young Investigator Award, a National Science Foundation CAREER Award, and a European Research Council Consolidator Award. Kochmann can be reached by email at dmk@ethz.ch.

Jonathan Hopkins is an associate professor of mechanical engineering at the University of California, Los Angeles, and the director of the Flexible Research Group. He received his PhD, master's, and bachelor's degrees all in mechanical engineering from the Massachusetts Institute of Technology, and conducted postdoctoral research at Lawrence Livermore National Laboratory. His current research focuses on enabling the design and fabrication of advanced flexible structures, mechanisms, and materials. His awards include the Presidential Early Career Award for Scientists and Engineers, The American Society of Mechanical Engineer's Freudenstein/General Motors Young Investigator Award, and the Watanabe Excellence in Research Award. Hopkins can be reached by email at hopkins@seas.ucla.edu.

Lorenzo Valdevit is a professor of materials science and engineering at the University of California, Irvine (UCI), and director of the Institute for Design and Manufacturing Innovation. He received his MS degree in materials engineering from the University of Trieste, Italy, in 2000, and his PhD degree in mechanical and aerospace engineering from Princeton University in 2005. His research focuses on modeling, optimal design, additive manufacturing, and experimental characterization of architected materials with superior combination of properties. His awards include the 2007 Faculty Award from IBM Corporation, the 2012 *Popular Mechanics* Breakthrough Award, and the 2018 Outstanding Faculty Service Award from the School of Engineering at UCI. Valdevit can be reached by email at valdevit@uci.edu.